JACS
JOURNAL OF THE AMERICAN CHEMICAL SOCIETY
Communication
pubs.acs.org/JACS

Electrochemical Imaging and Redox Interrogation of Surface Defects on Operating $SrTiO_3$ Photoelectrodes

Burton H. Simpson and Joaquín Rodríguez-López*

Department of Chemistry, University of Illinois at Urbana−Champaign, Urbana, Illinois 61801, United States

Supporting Information

ABSTRACT: We introduce electrochemical imaging and nano-resolved measurements of catalytic intermediates on operating $SrTiO_3$ photoelectrodes. Spatially resolved redox titrations of photogenerated reactive oxygen species (ROS) were used to profile changes in ROS coverage and reactivity at pristine and ion-milled defective areas on n-doped (100) $SrTiO_3$. Adsorbed ROS reached a potential-dependent limiting coverage of ∼0.1 monolayer and did not differ significantly between milled and pristine areas. However, the reaction kinetics between a solution-phase mediator and adsorbed ROS were found to be significantly decreased over ion-milled areas. Using a nanoelectrode, we resolved k_{si} values of 5 and 300 $m^3/s \cdot mol$ for these bimolecular reactions at defective and pristine sites, respectively. Ion-milled areas also showed significantly decreased activity toward photo-oxidations, providing evidence that photogenerated ROS mediate fast charge-transfer reactions with solution-phase species at the semiconductor−electrolyte interface. Our results provide spatially resolved direct evidence of the impact of surface defects on the performance of photoelectrochemical systems. Scanning electrochemical microscopy offers a powerful method for evaluating the reactivity of an operating electrochemical interface by using redox titrations that detected as few as 30 attomoles of adsorbed ROS.

Semiconductor photocatalysts use light as an energy input to drive uphill chemical reactions. This makes them an attractive option for implementing energetically expensive chemistries, such as producing sustainable fuels through water-splitting reactions,[1] advanced oxidation processes on waste-waters, or systems for pollutant photodegradation.[2] These require formation of highly reactive surface intermediates, such as trapped photogenerated holes and free or adsorbed reactive oxygen species (ROS).[2] Although many research efforts have been devoted to understanding how light excitation generates reactive holes (h^+) and electrons (e^-) in the bulk of the semiconductor,[3] chemical reactivity ultimately proceeds at the surface of the material.[4] Unraveling the spatial and temporal distribution of surface charge carriers and reactive species requires an *in situ* method that accesses distributions of local photoelectrocatalytic rates and surface intermediates at the micro- and nanoscales. Such studies will provide an unprecedented glimpse into the impact of surface-segregated redox processes, the role of surface imperfections and doping inhomogeneities on local photoelectrochemical (PEC) rates, and the synergy of surface co-catalysts with the semiconductor electrode.

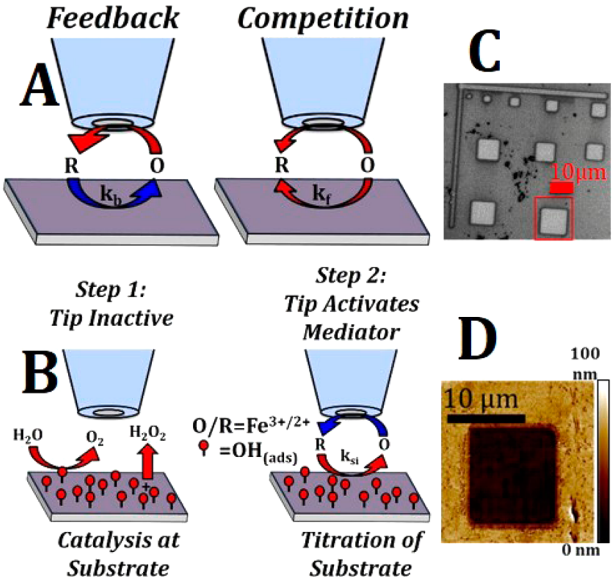

Figure 1. (A) In feedback mode SECM, the substrate cycles a mediator back to the tip. In competition mode, the substrate consumes the same species as the tip. (B) SI-SECM occurs in two steps: step 1 biases the substrate electrode to perform a catalytic reaction; step 2 generates a titrant at a UME to react with surface species. (C) Optical image of the milled pattern. (D) AFM image of of the largest square (red box in (C)).

We image a photoelectrocatalyst *in situ* using scanning electrochemical microscopy (SECM) and perform nanoscale redox titration of adsorbed intermediates through surface interrogation SECM (SI-SECM).We present the first *in situ* chemical imaging showing the impact of controlled surface defects on the distribution and reactivity of PEC surface processes on n-doped $SrTiO_3$ (STO) electrodes during water splitting. STO is a well-known photocatalyst with a bandgap that straddles the redox potentials of the hydrogen evolution reaction and the oxygen evolution reaction, making it highly active toward water splitting, even in the absence of potential bias.[5] Figure 1A depicts the use of a redox mediator to obtain steady-state SECM images of photocatalytic reactivity using the feedback and redox competition modes. In Figure 1B, SI-SECM is used to titrate persistently adsorbed ROS using transient feedback. We recently

Received: October 7, 2015
Published: November 13, 2015

DOI: 10.1021/jacs.5b10256
J. Am. Chem. Soc. 2015, 137, 14865−14868

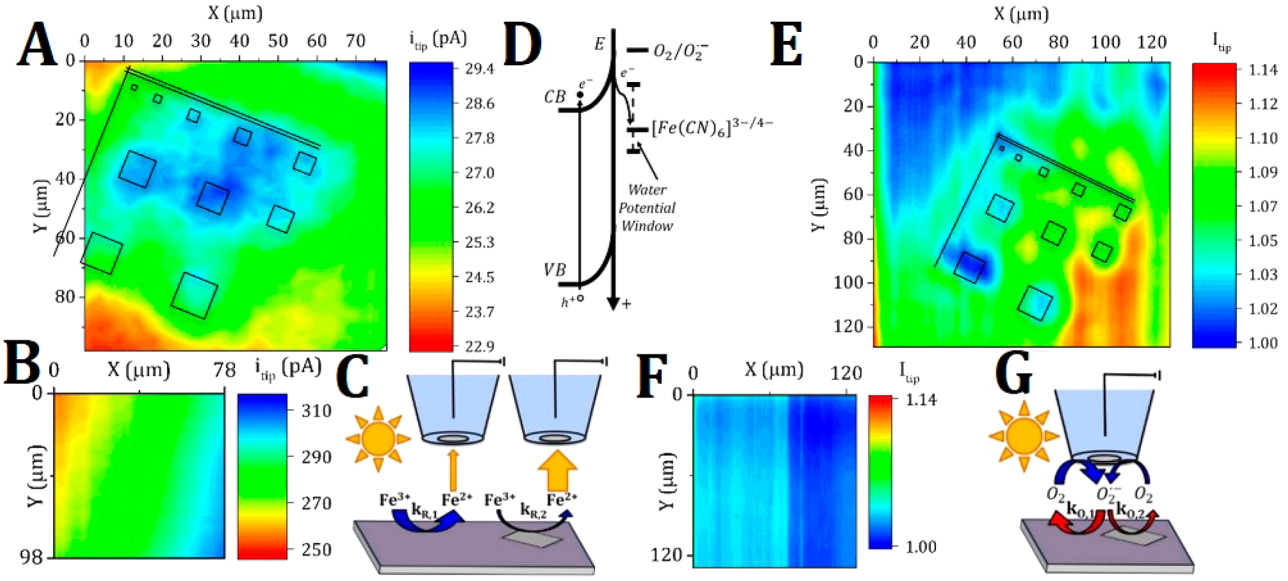

Figure 2. SECM images of the patterned area with the substrate at open circuit using a carbon UME ($a = 4\ \mu m$) positioned at $L = 1$ and biased to reduce the chosen mediator: Illuminated (A) and dark (B) 1 mM $K_3[Fe(CN)_6]$ in 0.1 M pH 9.3 borate buffer. Illuminated (E) and dark (F) 0.6 mM O_2 and 0.1 M TBA·PF_6 in DMF. Band diagram (D) and schematics illustrating the reactions occurring under illumination with the tip biased to reduce (C) $[Fe(CN)_6]^{3-}$ or (G) O_2 with the substrate at open circuit. A tilt-corrected version of (E) is available in the SI.

reported on the theory and experiment of SI-SECM redox titrations of ROS on STO photoelectrodes following photo-assisted water oxidation, using $[Fe(CN)_6]^{3-/4-}$ as redox mediator for SI-SECM.[6] In that work, we showed that a powerful feature of SI-SECM is its ability to simultaneously detect the surface coverage and chemical reactivity of adsorbed species, enabling a spatially resolved kinetic exploration of reactive adsorbates at surface features on operating photocatalysts.

Here, we demonstrate that localized surface defects created using focused ion beam (FIB) milling decrease the kinetics of photochemical oxidations in comparison to a pristine surface. For the first time, sub-μm-resolved SI-SECM is used to show that the reactivity of adsorbed ROS also exhibits a dramatic decrease on defective sites. This study supports the thesis that defects on photocatalysts give rise to lower efficiency of PEC transformations;[7] however, it furthers the quantitative investigation of the impact of mesoscale surface inhomogeneities on ROS formation and reactivity. This opens the door to exploring how co-catalyst interactions and hybrid photoelectrocatalyst[8] systems influence electrochemical rate constants of adsorbate-mediated charge transfers.

STO samples were prepared following the procedure thoroughly described in the Supporting Information (SI). Briefly, single-crystal (100) STO (MTI Corp., 10×10×1 mm, 1 side polished, made in Japan) was etched with 7:1 buffered oxide for 30 s and then annealed at 1050 °C under a constant H_2 flow to produce Ti-terminated STO with oxygen vacancies.[9] Mott−Schottky measurements showed that these samples were n-doped with a majority carrier concentration of 2.71×10^{20} cm^{-3} (see the SI). A rapid photoresponse was observed upon white light illumination, and IPCE measurements confirmed anodic photoactivity under UV illumination (see the SI). To create heterogeneities with controlled geometries, a gallium FIB milled the pattern in Figure 1C into the STO surface. AFM images (Figure 1D) showed that the patterned surfaces were 50 nm lower than the pristine STO surface. The RMS roughness of the milled areas was 3.03, somewhat higher than that of the pristine surface (2.59). All electrochemical measurements were done on a CHI920D SECM workstation (CH Instruments). For all experiments, a Ag/AgCl (3 M KCl) reference electrode was used, and a 1 mm diameter platinum wire was used as the counter electrode. PEC measurements used a 3-electrode configuration with STO as the working electrode. SECM experiments were performed with a 4-electrode configuration using either a 4 μm radius carbon fiber ultramicroelectrode (UME) or a 240 nm radius pyrolyzed carbon nanoelectrode prepared using previously described methods[10] as the working electrode and the STO as a second working electrode. Aqueous solutions were prepared in 100 mM borate buffer adjusted to pH 9.4 using NaOH. For all PEC measurements, a Xe arc lamp (6258 Oriel) illuminated the cell through an optical fiber.

SECM redox competition experiments, Figure 1A, revealed that FIB-milled patterns created on STO displayed a local decrease of photocatalytic activity. In this experiment, the SECM tip, positioned close to the unbiased and electrically isolated STO surface, competed for the reduction of bulk $[Fe(CN)_6]^{3-}$ to $[Fe(CN)_6]^{4-}$ at the inter-electrode gap. Since the standard reduction potential of the $[Fe(CN)_6]^{3-/4-}$ couple lies within the band gap of STO (Figure 2D), both h^+ and e^- can be transferred from the substrate to the mediator, even without external connections to the STO. The SECM tip current did not change in the dark, as the substrate was not active (Figure 2B). However, with the substrate free-standing at open circuit, illumination of the cell using white light decreased the observed $[Fe(CN)_6]^{3-}$ reduction current. Although significant diffusional broadening characteristic of the redox competition mode was observed, imaging the patterned substrate under these conditions revealed contrasting tip current between the patterned and pristine surfaces. The contrast aligned well with the pattern geometry (Figure 2A) and clearly displayed lower activity on features larger than the tip electrode. Illumination of the unbiased STO allows the mediator to equilibrate with the Fermi level of the semiconductor.[11] In this system, $[Fe(CN)_6]^{3-}$ is reduced to make the Nernst potential of the redox couple equal to the Fermi level of STO. Thus, the substrate competes with the tip to reduce $[Fe(CN)_6]^{3-}$, decreasing the tip current observed near the

DOI: 10.1021/jacs.5b10256
J. Am. Chem. Soc. 2015, 137, 14865−14868

substrate. This decrease suggests decreased reductive kinetics on the patterned surface as shown in Figure 2C, although other possibilities can be probed.

Reductive chemistry on $[Fe(CN)_6]^{3-/4-}$ at the free-standing STO substrate upon illumination requires a corresponding oxidation process. Possible oxidations include the re-oxidation of $[Fe(CN)6]^{4-}$ to $[Fe(CN)_6]^{3-}$ through a process similar to current doubling,[12] or the activation of water through oxygen evolution and the formation of intermediate ROS adsorbed on STO. These oxidations all have a common origin in reactive photogenerated h^+, which surface to react with water or the redox mediator. Damage from FIB treatment could increase $e^- - h^+$ recombination or decrease local doping, concomitantly affecting the generation of h^+. With this in mind, we explored differentiating the reactivity of oxidizing species at the STO surface.

The chemical reactivity of photogenerated h^+ can be isolated from that of adsorbed ROS by performing experiments in non-aqueous systems. In this case, we implemented SECM in the feedback mode using the $O_2/O_2^{\bullet-}$ pair as a redox mediator[13] in dried *N*,*N*-dimethylformamide. The standard reduction potential of $O_2/O_2^{\bullet-}$ lies negative of the band edge of STO (Figure 2D). This prevents the substrate from reducing O_2, so equilibration will not occur. However, local oxidation of tip-generated $O_2^{\bullet-}$ will occur by interaction with photogenerated h^+ at the surface of STO. Figure 2F shows that images taken by reducing O_2 at the tip electrode again show no contrast from the pattern without light. With the substrate at open circuit and unbiased, the tip current increases upon illumination when the tip is close to the substrate. This is termed positive feedback in SECM theory and demonstrates that the substrate oxidizes $O_2^{\bullet-}$ to O_2. SECM images under these conditions show less positive feedback on the pattern (Figure 2E), again indicating lower activity at the patterned sites. Evaluating the SECM tip current revealed a change in local kinetics from $k_f = 4.5 \times 10^{-4}$ m^2/s·mol for the pristine surface to $k_f = 2.5 \times 10^{-4}$ m^2/s·mol at the defective area. Together with experiments on the $[Fe(CN)_6]^{3-/4-}$ system, SECM feedback with $O_2/O_2^{\bullet-}$ confirmed that both e^- and h^+ reactivities at milled areas decrease with respect to the unmodified areas of the STO electrode.

Changes in the near-surface physical and electronic structures of STO due to ion milling are likely causes of the lowered activity. A several nm thick damage region containing a mix of amorphous and crystalline structures is expected as a result of recrystallization after beam-induced heating and Ga implantation.[14] Despite the post-milling etch step, some of this damage layer remains at the surface. Recrystallization allows relaxation of lattice defects from oxygen vacancies introduced during earlier processing. Using 30 kV accelerating voltage, Ga implantation is expected as far as 100 nm into the surface.[15] The increased secondary electron yield observed with low-voltage SEM (see the SI) at areas patterned by the beam suggests that these areas have a lowered n-type character compared to unpatterned areas.[16] Energy-dispersive X-ray spectroscopy on STO confirmed the presence of Ga at an FIB-milled area, but Ga was not detected on a pristine area (see the SI). These measurements suggest that, in addition to disrupting the physical structure of the STO surface, ion milling decreased the n-type character of the patterned regions. Together, these changes make the patterned areas less active toward photo-assisted oxidations.

We now turn to evaluating the reactivity of surface ROS. In the presence of water, adsorbed ROS will form on STO and remain persistently adsorbed after illumination is ceased in the absence of any reducing species. Adsorbed ROS play an important role in the selectivity and reactivity of anodic oxidation processes, just like the ones used in water remediation schemes and pollutant photodegradation. A fundamental question is if the defective surface created by FIB will affect the reactivity and quantity of these oxygen species on the surface. SI-SECM is a transient variation of SECM feedback that is especially well-suited to answer this question.[17] In this technique, as shown in Figure 1B, a SECM tip positioned near a substrate activates a mediator in solution to titrate reactive species on the substrate. Regeneration of the mediator by reaction with surface species gives positive feedback at the tip. From this current, the amount of reactive surface adsorbates can be measured. Simulations can be used to identify the bimolecular rate constant (k_{si}) governing charge transfer from the surface species to the titrant.[18] Recently, we demonstrated that simulations allow this technique to be applied at extended semiconducting surfaces.[6] This work also showed that the titrated area is well defined and controllable, allowing spatially resolved titrations on heterogeneous surfaces.

SI-SECM experiments were performed to understand whether the observed reactive heterogeneity corresponded to differences in adsorbed ROS coverage and reactivity. Titrations were performed in an aqueous solution of 50 μM $[Fe(CN)_6]^{3-}$ to optimize titration length and minimize light absorbance by the solution. During step 1 (Figure 1A), the STO was illuminated and biased to a potential positive of its flat band potential to activate the water oxidation reaction. For each site, a series of substrate biases from −0.3 to 0.3 V was used during this step. Titrations of photogenerated intermediates were performed in step 2 by reducing $[Fe(CN)_6]^{3-}$ to generate $[Fe(CN)_6]^{4-}$ as the titrant. Background SI-SECM transients measured immediately after each titration used the same substrate bias for step 1, but were performed without illumination. These backgrounds were subtracted from the respective titrations of photogenerated species to provide the interrogation currents used to extract reaction kinetics and surface coverage of ROS. Simulations used to fit experimental data followed the framework described in our previous publication.[6]

Figure 3A shows interrogation transients measured using a 4 μm radius carbon UME positioned at a distance of one tip radius above the surface. Interrogation of the pattern was performed in the middle of the largest individual square (red box, Figure 1C), while interrogations of the pristine surface were performed far from the pattern. Interrogations over the pristine surface fit well to simulations with a bimolecular rate constant of $k_{si} = 100$ m^3/s·mol, and showed a mostly stable surface coverage of ROS across the range of potentials tested (see the SI). In contrast, FIB patterned areas showed much slower kinetics, fitting simulations with $k_{si} = 10$ m^3/s·mol. The limiting coverage of ROS on the patterned surface, 0.083 ± 0.015 C/m^2, was more variable than on the pristine surface (0.05 ± 0.01 C/m^2), but the difference was statistically insignificant. This result is intriguing, suggesting that despite a lower activity of h^+, the surface coverage was comparable. Thus, there is intrinsically lower reactivity in the FIB damaged area. To discard the possibility that spatial variations affected the SI-SECM measurement, we dramatically increased our spatial resolution by introducing for the first time SI-SECM using nanoelectrodes.

To better differentiate adsorbate reactivity at the pristine or patterned surfaces, the same SI-SECM procedures were implemented using a carbon nanoelectrode tip (a = 240 nm, Figure 3B). Figure 3C shows interrogations performed above the pristine surface using the nanoelectrode and corresponding

DOI: 10.1021/jacs.5b10256
J. Am. Chem. Soc. 2015, 137, 14865−14868

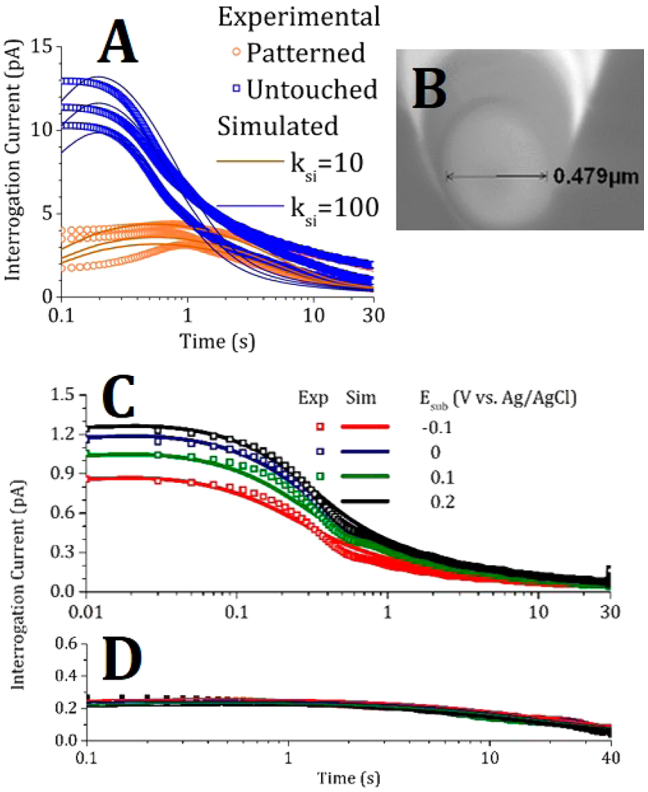

Figure 3. (A) SI-SECM titrations with an UME using $[Fe(CN)_6]^{3-/4-}$ after a photocatalytic step with the STO biased to +0.3 V vs Ag/AgCl and the simulated fits. Experimental data fit simulations using k_{si} = 10 or 100 m^3/mol·s for the patterned and pristine surface, respectively. (B) SEM image of a pyrolyzed carbon nanoelectrode used here. SI-SECM transients taken with a nanoelectrode (a = 250 nm) after photocatalytic steps on the pristine surface (C) fit well to k_{si} = 300 m^3/mol·s, but those at the pattern (D) fit k_{si} = 5 m^3/mol·s.

simulations that fit a bimolecular rate constant of k_{si} = 300 m^3/s·mol. These show a significantly better fit to simulated data than titrations with an UME. We think these better fits are likely due to less interference from tip electrode charging current and less heterogeneity in the interrogated area due to the smaller tip size (see the SI). In addition, the higher measured rate constant is likely due to the smaller tip−substrate distance allowing us to better challenge the fast kinetics of the bimolecular reaction at the substrate ($k_{et} \approx k_{si}\Gamma_A^\circ \approx 0.1$ cm/s). However, Figure 3D shows surface interrogations using the nanoelectrode on the pattern, and these fit to k_{si} = 5 m^3/s·mol, lower than observed with the UME.

This paper demonstrates the first application of redox nanotitrations by SI-SECM to characterize reactivity of adsorbed intermediates on a heterogeneous surface. Using a 240 nm radius nanoelectrode, we measured bimolecular rate constants for the reaction between our titrant and adsorbate of k_{si} = 300 and 5 m^3/s·mol on the pristine and defective surfaces, respectively. The dramatic difference in these rate constants shows that the modifications made to the surface directly influence the reactivity of photogenerated ROS. The observed differences seem to derive not only from changes in the PEC efficiency of different adsorbate species but also from changes in bonding energies at catalytic sites or other substrate−adsorbate interactions, currently under investigation in our laboratory.

■ ASSOCIATED CONTENT

Supporting Information

The Supporting Information is available free of charge on the ACS Publications website at DOI: 10.1021/jacs.5b10256.

STO preparation, profilometry data, photocatalyst characterization, and numerical simulations (PDF)

■ AUTHOR INFORMATION

Corresponding Author

*joaquinr@illinois.edu

Notes

The authors declare no competing financial interest.

■ ACKNOWLEDGMENTS

We acknowledge support from the Society of Analytical Chemists of Pittsburgh through a Starter Grant. Materials characterization was carried out in part in the Frederick Seitz Materials Research Laboratory Central Research Facilities, University of Illinois.

■ REFERENCES

(1) (a) Fujishima, A.; Zhang, X.; Tryk, D. A. *Int. J. Hydrogen Energy* **2007**, *32*, 2664. (b) Bard, A. J. *J. Am. Chem. Soc.* **2010**, *132*, 7559.

(2) (a) Diebold, U. *Surf. Sci. Rep.* **2003**, *48*, 53. (b) Fujishima, A.; Zhang, X. T.; Tryk, D. A. *Surf. Sci. Rep.* **2008**, *63*, 515.

(3) Nakamura, R.; Okamura, T.; Ohashi, N.; Imanishi, A.; Nakato, Y. *J. Am. Chem. Soc.* **2005**, *127*, 12975.

(4) (a) Wagner, F. T.; Somorjai, G. A. *J. Am. Chem. Soc.* **1980**, *102*, 5494. (b) Miyauchi, M.; Nakajima, A.; Fujishima, A.; Hashimoto, K.; Watanabe, T. *Chem. Mater.* **2000**, *12*, 3. (c) Xiang, Q. J.; Yu, J. G.; Wong, P. K. *J. Colloid Interface Sci.* **2011**, *357*, 163.

(5) (a) Mavroides, J. G.; Kafalas, J. A.; Kolesar, D. F. *Appl. Phys. Lett.* **1976**, *28*, 241. (b) Takeyasu, K.; Fukada, K.; Matsumoto, M.; Fukutani, K. *J. Phys.: Condens. Matter* **2013**, *25*, 162202.

(6) Simpson, B. H.; Rodríguez-López, J. *Electrochim. Acta* **2015**, *179*, 74.

(7) Gerischer, H. In *Photoeffects at Semiconductor-Electrolyte Interfaces*; Nozik, A., Ed.; ACS: Washington, DC, 1981; pp 1−16.

(8) (a) Giocondi, J. L.; Rohrer, G. S. *Chem. Mater.* **2001**, *13*, 241. (b) Choi, T.; Lee, S.; Choi, Y. J.; Kiryukhin, V.; Cheong, S. W. *Science* **2009**, *324*, 63. (c) Hong, K. S.; Xu, H. F.; Konishi, H.; Li, X. C. *J. Phys. Chem. Lett.* **2010**, *1*, 997.

(9) Wrighton, M. S.; Ellis, A. B.; Wolczanski, P. T.; Morse, D. L.; Abrahamson, H. B.; Ginley, D. S. *J. Am. Chem. Soc.* **1976**, *98*, 2774.

(10) Fan, F.-R. F.; Demaille, C. In *Scanning Electrochemical Microscopy*, 2nd ed.; Bard, A. J., Mirkin, M. V., Eds.; CRC Press: Boca Raton, FL, 2012; p 670.

(11) Nozik, A. J.; Memming, R. *J. Phys. Chem.* **1996**, *100*, 13061.

(12) Villarreal, T. L.; Gomez, R.; Neumann-Spallart, M.; Alonso-Vante, N.; Salvador, P. *J. Phys. Chem. B* **2004**, *108*, 15172.

(13) Zigah, D.; Wang, A. F.; Lagrost, C.; Hapiot, P. *J. Phys. Chem. B* **2009**, *113*, 2019.

(14) Rubanov, S.; Munroe, P. R. *Microsc. Microanal.* **2005**, *11*, 446.

(15) (a) Albrecht, J.; Leonhardt, S.; Spolenak, R.; Taffner, U.; Habermeier, H. U.; Schutz, G. *Surf. Sci.* **2003**, *547*, L847. (b) Saowadee, N.; Agersted, K.; Bowen, J. R. *J. Microsc.* **2012**, *246*, 279.

(16) El-Gomati, M.; Zaggout, F.; Jayacody, H.; Tear, S.; Wilson, K. *Surf. Interface Anal.* **2005**, *37*, 901.

(17) (a) Rodríguez-López, J.; Alpuche-Aviles, M. A.; Bard, A. J. *J. Am. Chem. Soc.* **2008**, *130*, 16985. (b) Park, H. S.; Leonard, K. C.; Bard, A. J. *J. Phys. Chem. C* **2013**, *117*, 12093.

(18) Rodríguez-López, J.; Minguzzi, A.; Bard, A. J. *J. Phys. Chem. C* **2010**, *114*, 18645.

DOI: 10.1021/jacs.5b10256
J. Am. Chem. Soc. 2015, 137, 14865−14868